CHARACTERIZATION OF MICROPHONICS IN THE cERL MAIN LINAC SUPERCONDUCTING CAVITIES

F. Qiu[1,2,†], S. Michizono[1,2], T. Miura[1,2], T. Matsumoto[1,2], D. Arakawa[1], H. Katagiri[1], E. Kako[1,2], H. Sakai[1,2], K. Umemori[1,2], T. Konomi[1,2], M. Egi[1,2]
[1]High Energy Accelerator Research Organization (KEK), Tsukuba, Ibaraki 305-0801, Japan
[2]The Graduate Univiersity for Advanced Studies (Sokendai), Hayama, Kanagawa 240-0193, Japan

Abstract

In the main linac (ML) of the KEK-cERL, two superconducting cavities with high loaded Q ($Q_L \approx 1\times10^7$) are operated in continuous wave (CW) mode. It is important to control and suppress the microphonics detuning owing to the low bandwidth of the cavities. We evaluated the background microphonics detuning by the low level radio frequency system during the beam operation. Interestingly, a "field level dependence microphonics" phenomenon was observed on one of the cavities in the ML. Several frequency components were suddenly excited if the cavity field is above a threshold field (~3 MV/m). We found that this threshold field is probably related with the cavity quench limits despite the unclear inherent physical mechanism. Furthermore, in order to optimize the cavity resonance control system for better microphonics rejection, we have measured the mechanical transfer function between the fast piezo tuner and cavity detuning. Finally, we validated this model by comparing the model response with actual system response.

INTRODUCTION

At KEK, a compact energy recovery linac (cERL) was constructed to study the feasibility of the future 3 GeV ERL based light source in 2009 [1]. It is a 1.3 GHz superconducting (SC) facility that operated in continuous-wave (CW) mode. In the main linac (ML) of the cERL, two nine-cell cavities (ML1 and ML2) were installed for energy recovery [2]. These two cavities have a high loaded Q (Q_L) of about 1×10^7, with the corresponding cavity half-bandwidth ($\omega_{0.5}$) of about 65 Hz. The lower bandwidth makes the cavity phase very sensitive to the microphonics detuning. A low level radio frequency (LLRF) system is usually required to reduce the microphonics effects.

Figure 1(a) compares the cumulative microphonics detuning as a function of the vibration frequency of the ML cavities in the past 5 years (indicated by different colors). In 2015, a 50 Hz component caused by scroll pumps was observed in both cavities (especially ML2). This components were disappeared after inserting a rubber sheet under the pumps. From 2016 to 2019, we have observed that the microphonics conditions gradually deteriorated in the ML1 cavity. Roughly, the RMS micrphonics detuning in 2019 (blue) is 2.5 times of the detuning in 2016 (red). On the other hand, such a phenomenon was not observed in the ML2 cavity. Figure 1(b) shows the corresponding RF stability (left: ML1, right: ML2) in the past 5 years. After 2016, according to Fig. 1(b), the RF stabilities for ML1 cavity were, unfortunately, getting worse due to the deteriorated microphonics conditions. Whereas the stabilities of ML2 cavity always performed well due to its similar microphonics conditions in the past five years.

In view of this situation, we have investigated the background microphonics of these two cavities carefully. Interestingly, a "field level dependence microphonics" phenomenon was observed in cavity ML1 [3]. We found that if the cavity field in the ML1 is larger than a threshold filed of 3 MV/m, several high frequency components were suddenly excited. This threshold field is probably related with quench limits according to the experimental results. Furthermore, in order to optimize the current resonance control, we measured the transfer function (TF) model between the piezo tuner and the cavity detuning, and then demonstrated the validation of the model in the beam commissioning. This paper will present our studies in 2019.

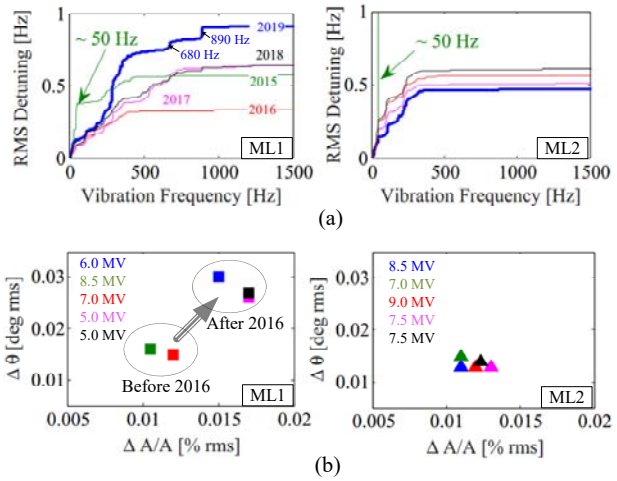

Figure 1: Five years comparison of (a) cumulative RMS detuning (in a function of vibration frequency) and (b) amplitude and phase stabilities (under feedback operation) of the ML1 (left) and ML2 (right). The cavity voltages in each operation are also marked in Fig. 1(b).

LLRF SYSTEM

Figure 2 shows the digital LLRF systems (indicated by red block) and frequency tuner system (indicated by blue block) of the ML cavities. The detailed information of these two systems can be found in [4-5] and [6], respectively. The phase differences ($\Delta\varphi$) between cavity pick-up and cavity incident (Pf) are calculated in both two systems. In LLRF system, this $\Delta\varphi$ will be further filtered

† qiufeng@post.kek.jp

by a first order low-pass filter with 2.5 kHz bandwidth to reduce the background noise. The microphonics detuning $\Delta\omega$ is then calibrated based on the $\Delta\varphi$ by the equation

$$\Delta\omega = \omega_{0.5} \cdot \tan(\Delta\varphi), \quad (1)$$

where $\omega_{0.5}$ represents the half-bandwidth of the cavity. In the tuner system, the $\Delta\varphi$ is first regulated by an integral (I) controller and then combined with a feedforward model (FF2 in Fig.2). This combined signal will finally drives a piezo tuner which tune the cavity resonance frequency.

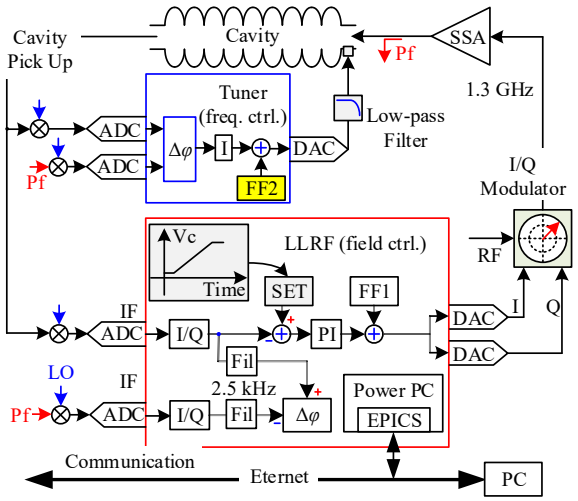

Figure 2: Schematic of the digital LLRF system (indicated by red block) and frequency tuner system (indicated by blue block) of the cERL ML cavity.

MICROPHONICS OF ML CAVITIES

In 2019, the operational field of ML1 was limited to 6 MV/m due to the degradation of the cavity performance [2]. We found that some high frequency components such as 680 Hz and 890 Hz were excited under 6 MV/m operation (see the accumulative RMS detuning plot at Fig.1). However, these components were disappeared when we operate the ML1 with lower field (e.g. 2 MV/m). It seems that the microphonics detuning is related with the field level in the ML1. To evaluate whether there is a field dependence of the microphonics detuning, we gradually increased the cavity voltage (V_c) by changing the set value of the LLRF system under feedback (FB) operation (see Fig. 2). The field-detuning map was then obtained by performing Fourier analysis of $\Delta\omega$ under different cavity field.

Figure 3 shows the measured field-detuning maps of ML1 (upper) and ML2 (lower) cavities. The color code here represents the detuning spectrum power. Interestingly, an unexpected boundary, corresponding to a threshold V_c of approximately 3.1 MV, was observed in the map of the ML1. Noted that the relationship between V_c and the cavity field (E_{acc}) is expressed as V_c [MV] = 1.038 [m]×E_{acc} [MV/m], i.e. the value of V_c and E_{acc} is almost same in our cavity [7]. In the field-detuning maps of the ML2, such a "field dependence microphonics" phenomenon did not appeared.

We scanned this field-detuning maps by several times under different LLRF conditions (switching on/off the LLRF FB control loops or the frequency tuner feedback loop). The threshold voltage was reproduced almost on the same value for all of these cases. We therefore ruled out the possibility of the FB loops that caused the "field dependency microphonics" phenomenon. On the other hand, we found the value of the threshold voltage is probably related with quench limits. The cavity quench limit field of ML1 was increased from 5.9 MV/m to 6.3 MV/m by the pulse (PS) aging processing. It is interesting to see that the threshold field was also increased from 3.0 MV/m to about 3.2 MV/m. After one week beam operation, we observed that the quench limits level was reduced slightly, as well as the corresponding threshold field. Table 1 has summarized the quench limits field and the corresponding threshold field under different stage [3].

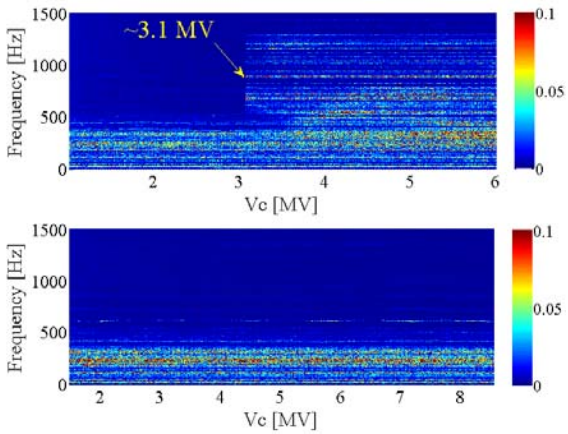

Figure 3: Field-detuning maps of ML1 (upper) and ML2 (lower) cavity. The color in the figure presents the intensity of the microphonics detuning. A threshold voltage of 3.1 MV appeared on the map of the ML1.

Table 1: Threshold Field versus Quench Limit Field

Cavity Conditions	Threshold E_{acc}	Quench Limits
Before PS aging	3.0 MV/m	5.9 MV/m
After PS aging	3.2 MV/m	6.3 MV/m
After one week operation	3.1 MV/m	6.1 MV/m

TRANSFER FUNCTION MEASUREMENT

In the current frequency tuner system based on I controller, the bandwidth of the closed system is less than several Hz. However, as shown in Fig. 3, the microphonics components are distributed from DC to several hundred Hz. That is to say, the current I controller is not capable of suppressing the microphonics detuning. To achieve a better performance of the tuner FB system, advanced control method such as active compensation method with adaptive finite impulse response filter or active noise control method are candidate approaches [8-9]. In such methods,

prior measurement of the tuner TF model is necessary (or helpful) for the controller design.

The TF model of piezo tuner system with N modes is given by [8]

$$H(s)=\left(\frac{M_0}{\tau s+1}+\sum_{k=1}^{N}\frac{\omega_k^2 M_k}{s^2+2\xi_k\omega_k s+\omega_k^2}\right)e^{-T_d s}. \quad (2)$$

The parameter M_0 is the steady state gain and τ a time constant of a low-pass filter. The parameter T_d represents the group delay of the system. The parameters ω_k, M_k and ξ_k represent the frequency, magnitude, and damping constant of the kth mode, respectively.

In cERL, inspired by the successful experience of a disturbance observer (DOB)-based method in the LLRF field control system [5], we also estimated the possibility of extending this method to the tuner control system in 2016 [6]. A tuner system model is also required in the design of the DOB-based controller. However, due to the time limitation in the beam commissioning, we did not have enough time to measure the complete TF model of the tuner system at that time. We only considered that the tuner system is a simple first-order model [see the first order model in (2)] with a group delay, and then used this simplified model for controller design. The experiment is not fully successful due to the oscillation of a 340 Hz mechanical mode [6].

In 2019, we have measured the tuner TF by exciting the tuner system with the sinusoidal signal from FF2 (see the yellow block in Fig. 3). The response of the cavity detuning was then calculated by LLRF system. We recorded the response of the tuner system from 5 Hz to about 340 Hz which covers the main vibration components. The frequency step is set to 1 Hz, and for each frequency point, up to 5 seconds measurements was conducted to achieve a steady state response.

The amplitude and phase response of the tuner system of ML1 (blue) and ML2 (red) are shown Fig. 4. From the amplitude response of ML1, a 340 Hz mechanical mode is easily found. This mode is in good consistence with the result in Ref. [6]. In addition, for ML1 tuner system, the steady state gain M_0 is approximately 2.6 according to Fig. 4. This result is also in good agreement with the result in Ref. [6], which has a M_0 of 2.7. By fitting a linear curve to the phase response plot, we can identified the system group delay of 0.11 ms by the slope of the linear curve. The other parameters in each mechanical mode can be identified by modern system identification method.

To validate the identified TF model, we have compared the response of the TF model and actual tuner system in the ML1 cavity. Firstly, we operated the tuner system and LLRF system with the open-loop. In the next step, we excited the tuner system with two types of signals, type-A and type-B. In the case of the type-A, the excited signal is a 50 Hz square wave signal with amplitude a_1. In the case of the type-B, the excited signal is a 20 Hz square-wave with the amplitude $4{\cdot}a_1$. Finally, we measured the corresponding cavity detuning response of this two cases.

Figure 5(a) has compared the response of the type-A signal of the actual system (indicated by blue color) and the TF model (indicated by red color). Similarly, Figure 5(b) compared the responses of the type-B signal. The results are in good agreement in both of these two cases.

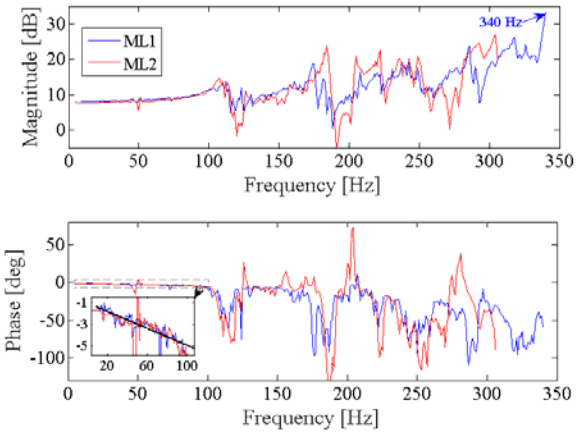

Figure 4: Tuner amplitude (upper) and phase (lower) response as a function of exciting frequency of ML1 (blue) and ML2 (red).

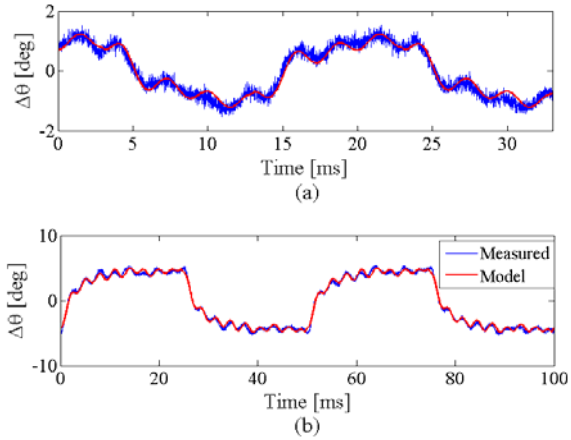

Figure 5: Comparison of the square-wave response of the transfer function model (red) and actual tuner system (blue). We have applied two types of square wave. (a) Type-A, 50 Hz and amplitude = a_1, (b) Type-B, 20 Hz and amplitude = $4{\cdot}a_1$.

SUMMARY

The microphonics detuning is increased in the past five years in one of the ML cavities. After investigating the cavity back-ground microphonics carefully, a "field level dependency microphonics" phenomenon was observed. Several components were suddenly appeared if the cavity field is above a threshold field of 3 MV/m. This threshold field is probably related with the quench limits although the internal mechanism is still not well understood. Furthermore, we have measured the TF model of the tuner system, and then validate the model by comparing the model response with the measured system response. For the future work, we will optimize our tuner control with the identified TF model.

REFERENCES

[1] M. Akemoto *et al*., "Construction and commissioning of compact energy-recovery linac at KEK", *Nucl. Instr. Meth.*, vol. 877, pp. 197-219, 2018. doi:10.1016/j.nima.2017.08.051

[2] H. Sakai *et al*., "Long-term operation with Beam and Cavity Performance Degradation in Compact-ERL Main Linac at KEK", in *Proc. LINAC'18*, Beijing, China, Sep. 2018, pp. 695-698. doi: 10.18429/JACoW-LINAC2018-THPO008

[3] F. Qiu *et al*., "Status of microphonics on cERL nine-cell cavities" in *Proc. PASJ2019*, Kyoto, Japan, July-Aug. 2019, paper: WEPH010.

[4] T. Miura *et al*., "Low-Level LLRF system for cERL", in *Proc. IPAC'10*, Kyoto, Japan, May 2010, pp. 1440-1442, paper: TUPEA048

[5] F. Qiu *et al*., "Application of disturbance observer-based control in low-level radio-frequency system in a compact energy recovery linac at KEK", *Phys. Rev. ST Accel. Beams*, vol. 18, p. 092801, Sep. 2015. doi: 10.1103/PhysRevSTAB.18.092801

[6] F. Qiu *et al*., "Progress in the work on the Tuner control system of the cERL at KEK", in *Proc. IPAC'16*, Busan, Korea, May 2016. Pp.2742-2745. doi: 10.18429/JACoW-IPAC2016-WEPOR033

[7] H. Sakai *et al*., "Field emission studies in vertical test and during cryomodule operation using precise x-ray mapping system", *Phys. Rev. Accel. Beams*, vol. 22, p. 022002, Feb. 2019. doi: 10.1103/PhysRevAccelBeams.22.022002

[8] A. Neumann *et al*., "Analysis and active compensation of microphonics in continuous wave narrow-bandwidth superconducting cavities", *Phys. Rev. ST Accel. Beams*, vol. 13, p. 082001, Aug. 2010. doi: 10.1103/PhysRevSTAB.13.082001

[9] N. Banerjee *et al*., "Active compensation of microphonics detuning in high Q_L cavities", *Phys. Rev. Accel. Beams*, vol. 22, p. 052002, May 2019. doi: 10.1103/PhysRevAccelBeams.22.052002